IIETA International Information and Engineering Technology Association
Advancing the World of Information and Engineering

Mathematical Modelling of Engineering Problems
Vol. 12, No. 7, July, 2025, pp. 2234-2244
Journal homepage: http://iieta.org/journals/mmep

Evaluation of the Effect of Nano Al_2O_3 Additive on Al-Si-Cu Alloys Performance Produced by Squeeze Casting and High Pressure Die Castings: Experimentation and Mathematical Modeling

H. Ali Hussein[1], Suhair G. Hussein[2*], Bassim Bachy[2]

[1] Production Engineering and Metallurgy Department, University of Technology, Baghdad 19006, Iraq
[2] Department of Mechanical, College of Engineering, University of Baghdad, Baghdad 47024, Iraq

Corresponding Author Email: suhair.g.hussein@coeng.uobaghdad.edu.iq

https://doi.org/10.18280/mmep.120704

Received: 30 January 2025
Revised: 22 April 2025
Accepted: 30 April 2025
Available online: 31 July 2025

Keywords:
modelling, design of experiments (DoE), squeeze casting, high pressure die casting (HPDC), wear resistance, mechanical properties, nano-Al_2O_3, corrosion behavior

ABSTRACT

Light alloy metals (Hypoeutectic Al-Si-Cu alloys) have retained their importance and properties as primary candidates when examining the correlation of the cost function that makes them suitable for many applications. The research aims to fabricate Al-Si-Cu alloys using nano-Al_2O_3 as heterogeneous nucleation of a eutectic solution to appropriately squeeze casting and pressure die casting processes under varying pressures (150, 200, and 250 MPa), pouring temperature with 780°C, mold preheated to 250°C. The yield strength and elongation are 12%, and also the hardness is 33.1% higher than that of gravity castings. In addition, the samples from the squeeze casts have lower wear rates than the samples of the pressure die cast. The design of experiments (DOE) method was applied to study and monitor the properties of Al-Si alloy. The relationship between the process parameters, including casting pressure and the percentages of Nano additives, and the main process responses was analyzed. Based on the used modeling tool, the final equations of the responses, including hardness, corrosion, tensile strength, and wear rate, were found. The modeling results showed good agreement with the experimental results, with a maximum error of 1.54% and a minimum error of 0.25%.

1. INTRODUCTION

Aluminum alloys are used more frequently than magnesium alloys because of their high resistance to corrosion and the pressing need for lightweight transportation. Unfortunately, the commonly used die-cast aluminum alloys invariably have yield strengths (YS) in the 90–170 MPa range. raise die-cast Al alloys' as-cast YS by routine alloy composition modification, but the gains were not particularly noteworthy since the die-cast Al alloys' YS is still below 190 MPa in accordance with 4% industrially acceptable ductility in standard tensile samples. Due to the efficiency of strengthening, particle strengthening may be a viable option for die-cast Al alloys to obtain high strength in as-cast state. Stronger materials are produced by nanoscale particles' efficient inhibition of dislocation movement and induction of grain refinement. This improvement is essential for uses where materials must be able to sustain heavy loads and pressures. Stronger and lighter materials can help save energy in machinery and transportation, supporting international initiatives for sustainability and lower carbon footprints [1, 2].

Advanced squeeze casting (SC) techniques [3, 4] can be considered a promising and appealing solution for the automotive industry in this context. Furthermore, this process allows for the use of wrought alloys, which are typically high-performance alloys that could previously only be developed through forging. The working cycle is similar to that of high pressure die casting (HPDC). A shot sleeve is used to inject melts of aluminum alloy into steel die holes [1, 3]. Because HPDC components blister after solution heat treatment, most HPDC parts in industry are made using conventional non-vacuum processes and are therefore unsuitable for further fortification by solution and aging heat treatment [4, 5]. Heat treated die-castings can be produced using the recently invented vacuum-assisted HPDC, however the process requires more time and energy [6, 7]. As a result, as-cast usage is suggested for the majority of HPDC components, but all of the finishing operations are eliminated [5, 6].

Various studies have focused on the Microstructure has an impact on the mechanical properties of metallic alloys, particularly dendrite arm spacing and corrosion behaviour relationships [1, 2]. Silicon is the most common alloying element in aluminium castings; it provides superior castability and weldability due to high fluidity and minimal shrinkage [3, 7]. This is due to silicon's exceptional effect in improving casting characteristics, as well as other physical properties. Structure modification in the naturally occurring eutectic can significantly improve the mechanical properties of aluminum alloys. In general, alloys containing 5% Si up to the eutectic concentration are considered to be eutectic [5, 6] provide the best results. The impacts of process parameters are significant because the structure and characteristics of alloys can be

enhanced by introducing trace quantities of nano-Al_2O_3 components. The designers were able to understand the importance of the elements that will eventually affect the design of the finished product by employing the design of experiments (DoE) technique. The DoE tools have been used intensively in many applications and fields such as manufacturing including laser cutting [8], drilling [9], and welding [10]. Numerous research has examined the DoE method's use, and the results have been noteworthy advancements in science of computer. Many researchers [11] have used the DoE approach to study the behavior of alloys based on aluminum. These researchers discovered that the workpiece's strength and composition had the most impacts on tool life. A model developed by Xing et al. [12] and Othman et al. [13] showed that the torque and thrust force required to drill the last hole are about 50% more than those required to drill the first.

The mechanical and physical characteristics of Al-Si-Cu alloys can be greatly impacted by nano-Al_2O_3 (alumina) reinforcement. Here is an overview of the main consequences:

Al-Si-Cu alloys' mechanical and physical characteristics are greatly influenced by nano- Al_2O_3 (alumina) reinforcement, which fines the grain structure during solidification to produce finer microstructural characteristics. Reduce clustering or segregation by distributing the alloy matrix more evenly. makes them more wear-resistant by increasing the yield strength and ultimate tensile strength through strengthening mechanisms such load transfer, strengthening, and grain boundary strengthening. It also rises with the addition of nano-Al_2O_3. Boost the alloy's thermal stability to reduce its susceptibility to thermal deterioration at high temperatures. Increase Al-Si-Cu alloys' resistance to corrosion by erecting a barrier against external influences. Changing the viscosity of the alloy can improve fluidity during casting, which improves mold filling and lowers flaws.

The goal of this study was to examine how pressure and nano-Al_2O_3 influenced the macrostructure, mechanical characteristics, and corrosion behavior of aluminium-silicon-copper alloys formed via squeeze casting and high-pressure die-casting. The data were analyzed using a two-factor, three-level complete factorial design. To determine the link between the factors under investigation, a process was created by integrating the relevant between the process parameters such as nano-percentage additives and the pressure with the main responses including microstructure, mechanical characteristics, and corrosion behavior of both squeeze casting and HPDC casting.

2. EXPERIMENTAL METHOD

2.1 Modifier preparation

The additives are made in the form of granules or tablets, consisting of 1 gram of pure aluminium powder (250 μm) mixed with 0.1wt% nano-Al_2O_3 and pressed at 150 bar to make tablets (10 mm dimeter × thickness 9 mm) that are simples to handle while also enhancing oxidation resistance and avoiding floating.

2.2 Casting techniques

The chemical makeup of the Al-Si-Cu alloy employed in this investigation is displayed in Table 1. In the case of an electric furnace, the charge alloy Al-Si-Cu was heated to 780℃ (Carbolite, England 5 kg). Then 3 liters per minute of inert gas (argon) was pumped after heating to 400 degrees Celsius during the mixing process until reaching the pouring process to remove the gas from the chamber., Synchronized with mechanical stirring at 400 rpm by high-speed steel propeller (three blades). Before being added the nano-Al_2O_3 to the molten alloy, elements were heated to 150℃ to remove moisture. Nano-Al_2O_3 with particle sizes of 30-50 nm (0.3-0.7 percent) was added to alloy. The molten agitation was carried out for around two minutes in order to encourage homogeneous dispersion of the reinforcing and wetting nuclation. The molten alloy was 780℃ then poured into each high speed steel mold (H.S.S) then pressed in different pressure as shown in Table 2, which was preheated to 300℃ (20 mm in diameter and 120 mm in length), as seen in Figure 1. Table 2 lists the process parameters that have been set up after pre-experiments.

Table 1. The Al-Si-Cu alloy's chemical composition (in weight percent)

El.	Cu.	Si.	Zn.	Mn.	Fe.	Mg.	Ni.	Ti.	Cr	Al
wt.%	3.78	8.2	0.44	0.15	0.61	0.07	0.11	0.09	0.003	Rest.

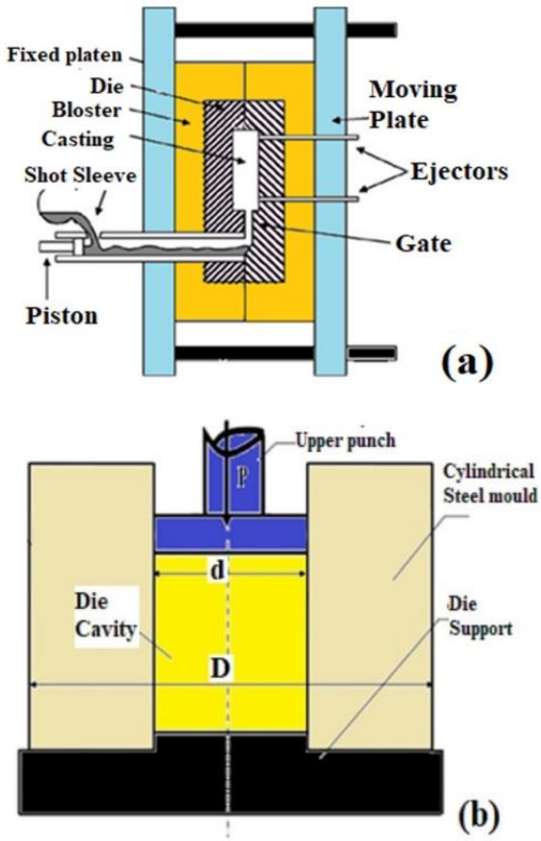

Figure 1. Schematic diagram of (a) pressure die cast and (b) squeeze casting test

Table 2. The limits and parameters of the process

Units	Limits		
	-1	0	1
%	0.3	0.5	0.7
MPa	150	200	250

2.3 Experimental measurements and tests

2.3.1 Microstructural analysis

Optical and utilized an X-ray diffraction Shimadzu (XRD6000) diffractometer to study the phases of modified Mg AZ91 alloy samples. The radius scanning is 185 mm, C, and NF (154060 nm) radio X-rays, and the radius leakage is less than 2.5 Sv/h.

Image-J analysis tools uses color contrast to separate items from the background and aids in the identification of individual particles. This software allows you to identify and measure properties such as area, volume fraction, and particle size on a scale. At the highest output. microstructure images were prepared by grinding with 320.0, 600.0, 800.0, 1000.0 and 1200.0 granular papers, respectively. The samples were polished by alumina, washed with alcohol, and etched by Killer's solution. A mixture of 5 ml NHO_3, 3.0 ml HCl, 2.0 ml HF, and 190.0 ml H_2O.

2.3.2 Hardness test

Vickers device was used to test the hardness (type ZWICK-Z323 - Germany). The applied load is (0.5 kg) for ten seconds, and the chemical make-up of the Al-Si-Cu alloy used in this experiment (in weight percent).

$$HV = 1.8544 * \frac{P}{\left(D_{AV}\right)^2} \quad (1)$$

where, HV stands for Vickers hardness, P stands for applied load (gr), and D_{AV} stands for diagonal length (mm).

2.3.3 Corrosion tests

The electrochemical analysis and cyclic polarization of Cu-Al-Si alloys were tested using a computer-controlled (P.C.I.4/750-G.A.M.R.Y, Inc., Warminster-P.A) device. Expose all experiments in 3.5% NaCl solution. At a temperature of 25 degrees Celsius. Ag/AgCl is used as the reference electrode and the auxiliary-electrode made of noble metal (Pt) and for the working-electrode is used as the sample holder. The exposure area is 10 mm^2. Before testing, the surface of the samples is prepared with metallographic polishing. The first stage is the open circuit voltage (OCP) check. The second stage is to test the cyclic polarization after determining the open circuit voltage. All data is determined by surface area. It is calculated using the Echem-analyzer to optimally determine the outcome [12, 13].

2.3.4 Wear test analysis

At room temperature, dry tests were conducted using ASTM F732-82 and a pin and disc test [14]. 1o mm and 1o mm long Al-Si alloy modified nails were polished with different grain size sand sheet (22o, 32o, 5oo, 8oo, 1ooo), cleaned ay alcohol, and dried. The instrument device is made up of a motor that rotates at a constant speed (510 rpm). The dial is made of tool steel that has a 65 HRC hardness. Relative mass changes were calculated by weighing samples before and after use using a digital sensitivity scale rating scale (DENVER) equipment, Japan (maximum 210 g) of 0.0001 mg. Five N was the load. Cleaning of the disk is done after every test. To calculate wear, the equation below is used.

$$\text{Wear rate} = \frac{\Delta W}{S} \quad (2)$$

$$S = V * t \quad (3)$$

$$V = \frac{\pi \cdot DN}{1000 * 60} \quad (4)$$

where, W: weight of sample before, and after the test (gm), D: diameter (m) of 0.14, S: sliding distance (m), N: r.p.m of 510, V: velocity (m / sec), t: time (Sec).

2.3.5 The tensile strength measurements

The tensile test values were measured using the prepared samples according to ASTM (E8M) standard, type Instron (WDW - 200E) used to test the samples.

3. RESULTS AND DISCUSSION

3.1 Experimental results

3.1.1 Metallographic studies

Modifying the microstructure with ceramic nano reinforcements significantly improves the properties of aluminum matrix composites (AMCs). When added in conventional particle form, ceramics typically do not wet well with molten aluminum. This leads to agglomeration of the reinforcements and, consequently, poor distribution, which severely degrades the property improvement. The in-situ formation of ceramic nanocomposites has several advantages, such as uniform spherical matrix density, no reinforcement lift, and excellent physical and chemical properties [5]. A suitable method can produce low- or pure-form in situ nanocomposites with a uniform and integrated microstructure, even in practical applications. Various processes, such as reactive particle leaching and self-diffusion synthesis at high pressure and temperature, are being investigated to produce in situ nanocomposites. Characterization of these composites using complex techniques enables a deeper understanding of interface interactions and chemical bonding between the matrix and reinforcements. The mechanical behavior and high-compression performance of in situ nanocomposites significantly outperform their conventional counterparts, thanks to the high reinforcement aspect ratio and optimal load transfer efficiency. Analysis indicates that the elastic modulus of in situ composites can significantly increase with increasing volumetric ratio of reinforcements, exhibiting a largely positive linear relationship with the reinforcements due to the significant reduction in plastic deformation in the matrix [9].

Figure 2 illustrates the experience of another cooling rate microstructure that shows the eutectic silicon continues to nucleate on the dendrite. The field of concern is extended in Figure 2. The eutectic silicon platelet (1) begins to expand from a dendrite limb. The red curve indicates the boundary between the dendrite arm and the eutectic area in the expanded portion. (2) In the eutectic, tends to rise from aluminum. Therefore, in the eutectic, it seems that silicon could also nucleate in the eutectic on the aluminum. Area (3) is in the eutectic, aluminum.

A series of squeeze casting trials was performed for an Al-Si-Cu aluminum alloy with Al_2O_3 nano-sized particles of 0.3, 0.4, and 0.5 wt% content by controlled crystallization. Structure and mechanical properties were studied. It was established that a low content of nanoparticles increased the ultimate tensile strength by 40% and had a bracing effect on the Si flakes. It is shown that the increase in casting strength

was connected to the higher content of uniformly distributed regular eutectic crystals with a suppression of the refining of α-Al grains. Herein, a series of squeeze casting exercises was carried out, using the nano-sized Al_2O_3 powder in the liquid metal, prepared earlier from aluminum alloys [14].

The microstructure of the cast samples was found to be solid solution of aluminium (α) and eutectic (α+Si) in all cases, according to the results of metallographic studies. In Figure 2, the grain sizes for as cast are equal to 27.56 µm, on the other hand, varied depending on the casting variable [13, 14].

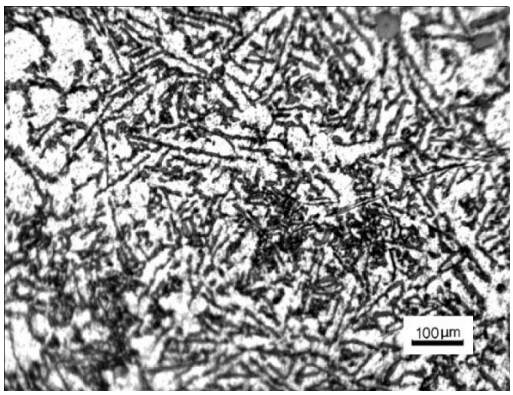

Figure 2. Gravity castings of Al-Si-Cu alloy micrograph

The results of a pressures MPa effect of Aluminium dendrites microstructure in squeeze castings have been discovered to be finer than those in high pressure die-castings, The smallest mean size of the grain was obtained with the addition of 0.7% of Al_2O_3 for all applied pressures. The average grain size of SQ casting was 10.08 µm, 7.621 µm, and 4.682 µm, respectively. And the average grain size of HPDC casting was 10.817 µm, 9.211 µm, and 6.012 µm, respectively. with the fineness grin size decreasing as the squeeze pressure increased, as shown in Figures 3(A)-(C) with the structure being finer than that high pressure die cast in Figures 3(D)-(F). Squeeze cast products' grain sizes (ASTM grain size number) are determined by pressure. The increased pressure of each process did result in any significant refinement due to the high cooling rate and heterogonous nucleation by Al_2O_3 [5, 15].

During the solidification of hypoeutectic alloys, In the molten alloy, Al_2Cu and Al_2O_3 particles may serve as diverse nucleating sites for eutectic aluminum refining and eutectic silicon particle modification [16]. Si has far too many misfits with the two most common Al_2O_3 types to act as a heterogeneous nucleate for the oxides. Al_2O_3 nanoparticles can be used to refine and modify Si shape in hypoeutectic Al-Si alloy melts at the same time. Eutectic silicon and α-Aluminum dendrites exhibit reduced grain size. Furthermore, the modifying impact is greatly boosted when the Al_2O_3 concentration is increased by 0.7% as shown in Figure 3 [17].

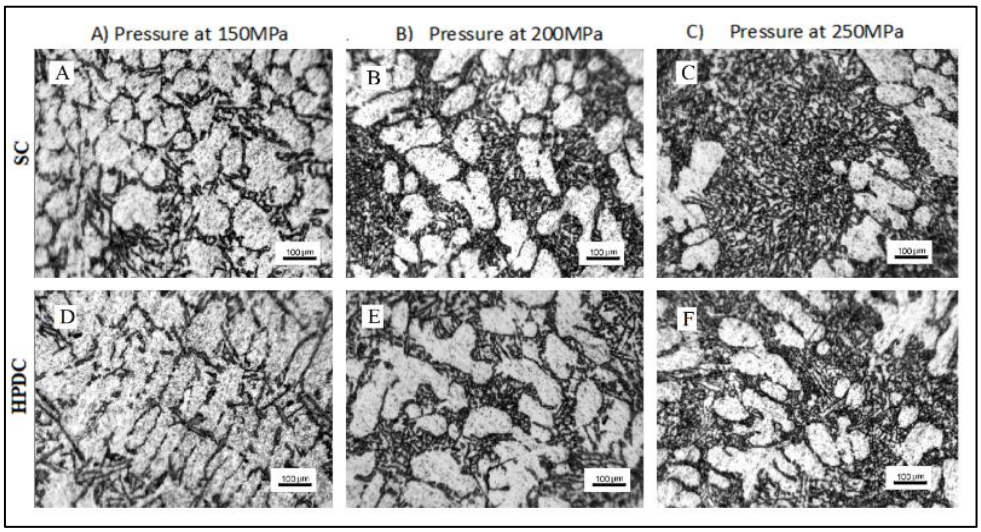

Figure 3. Micrograph of SC and HPDC of Al-Si-Cu alloy modification by 0.7% Al_2O_3

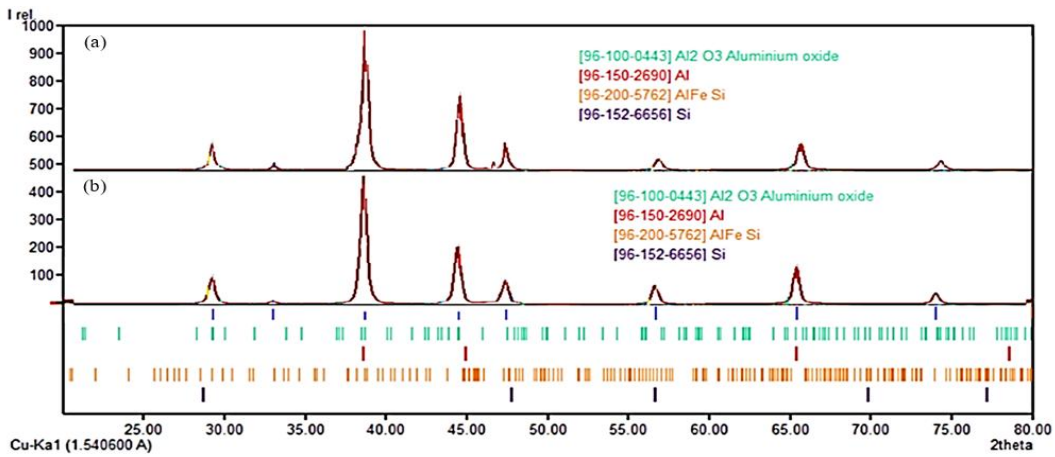

Figure 4. XRD pattern of SQ and HPDC-processed Al-Si-Cu samples

In Figures 4(a) and (b), the XRD pattern of Al-Si samples treated by SQ alloy and HPDC is displayed. The unique Al-Si alloy is discovered to consist of four phases, including α-Al, AlFeSi, and the Al_2Cu phase. Si; diffraction peaks associated with Al_2O_3 and Al compounds are detected, as expected, which means that the phase react with aluminum and silicon completely to form and Al_2O_3 particles by an in-situ melt reaction. Figures 3(A) and (B) show the diffraction lines and exhibits peaks of Al_2O_3 at 12.43°, 34.54°, 65.61° and 69.46°, corresponding to the 001, 011, 210 and 040 reflections of face-centered cubic. The acquired diffraction pattern has not found to be matching the calculated patterns standard chart, because the nano-dopant element consists only of aluminum and phosphate [14].

3.1.2 Hardness

At various applied pressure, Figure 5 depicts the relationship between the hardness and applied pressure. The Al-Si-Cu alloy's hardness increased from Hv 87.28 Kgf for cast without pressure to Hv 135.52 for squeeze castings and Hv 129.43 for high pressure die castings, a 37 per cent hardness increase for a cast pressure. Squeeze cast products have a higher hardness because of Al_2O_3 and Al_2Cu particles, which cause grain refinement and the elimination of porosity. Certainly, reduces the volume of microporosities in the matrix. Dislocations cannot move through complicated phases such as intermetallic phases, Al_2O_3 and silicon particles during the test [17].

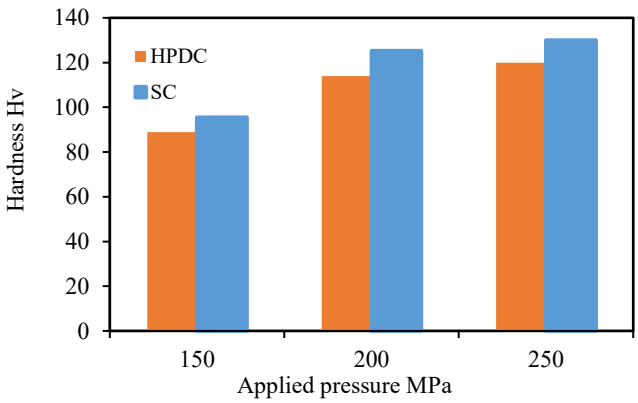

Figure 5. Micro hardness of SC and HPDC of Al-Si-Cu alloy

3.1.3 Electrochemical characterization

Al-Si-Cu alloy samples cast at pressure and high pressure in 3.5 M NaCl solution at 25°C are displayed in Figure 6 along with their dynamic effective polarization curves. With SC samples exhibiting a decreased corrosion rate, our findings corroborate the corrosion resistance trend found when comparing experimental and simulated plots for Al-Si-Cu alloys. When compared to the findings of cast samples, the pressure casting parameter significantly shifted the corrosion potential to the noble side and decreased the corrosion current density by almost 100 mV. Even though HPDC generated the samples, Figures 6(a) and (b) [18] show that the anodic curve morphologies are on the noble side and somewhat different from as cast.

As the content of the nano-Al_2O_3 was increased in the samples, the anodic curves over the polarization potential were shifted to more negative values, which means that the corrosion potential of the HPDC samples was more positive than that of the SQ cast alloy. Furthermore, it was found that as the content of the nano-Al_2O_3 was raised to 0.7 wt%, the anodic polarization curves began to rise, which indicated a significant enhancement of the corrosion resistance of the composites against corrosion. At a certain nanoscale reinforcement content in the composite, a small number of nano-Al_2O_3 particles had little contribution to the formation of the corrosion resistance, while high contents might induce large agglomeration of additives due to high viscosity, which worsens the defects in the corrosion resistance [18].

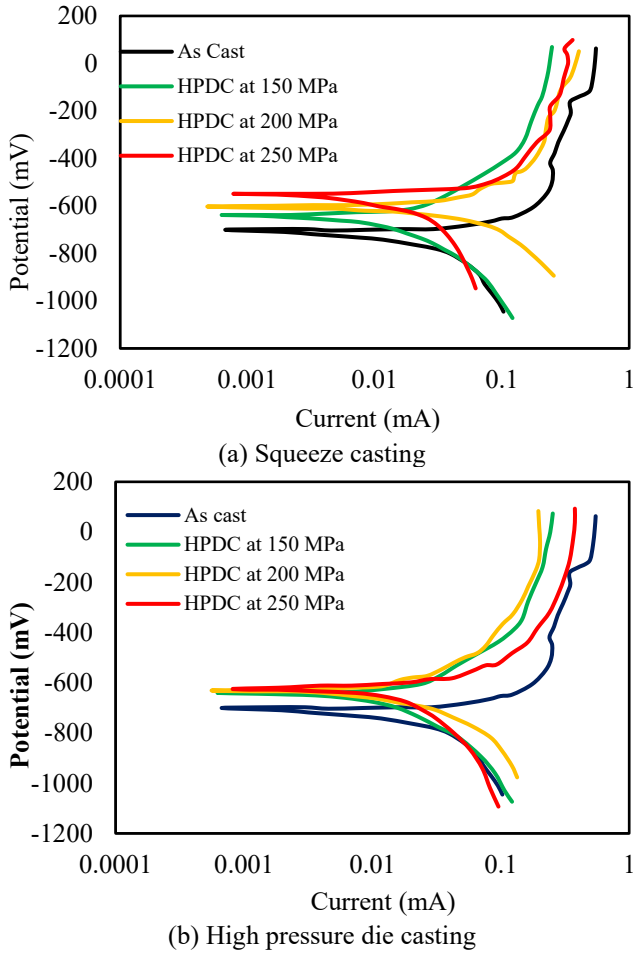

Figure 6. The impact of high pressure die cast and pressure squeeze casting on corrosion behavior is seen by the polarization curve

In this case, the increase in the boundary between the (α) phase and the Si particles, which grow in different ways, is linked to a reduction in corrosion resistance caused by the SC process and HPDC [17, 18]. Due to a specific deformation in the atomic plane, the boundaries are completely incompatible, particularly on the Al-rich phase side of the interface, where the phase hardens with stiff surfaces and Si develops faceted from melting (growing of smooth interface). This localized deformation increases the regularity of the microstructure, which results in regular corrosion of the structures [19, 20].

The low-weight contents of additional Al_2O_3 nanoparticles can stabilize the passive coatings generated on the alloy surfaces. However, with sufficient Al_2O_3 nanoparticles, deterioration of the passive coatings develops, so that the alloy exhibits high corrosion susceptibility [20, 21]. It can reduce galvanic corrosion on the alloy surface in addition to noble AlO_3. Al-Si-Cu alloy's mechanical and corrosion resistance are improved by the addition of AlO_3 nanoparticles [18].

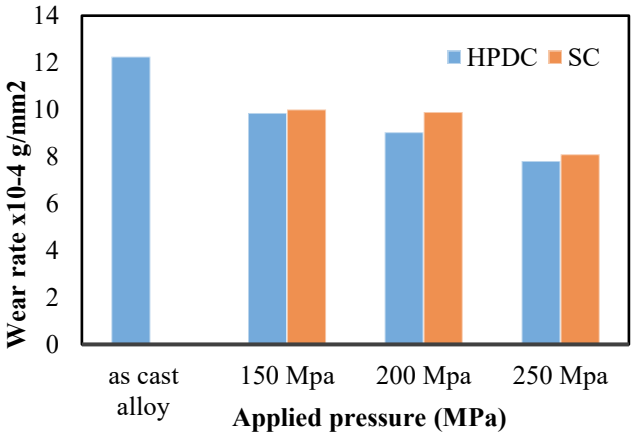

Figure 7. The effect of applied pressure on the wear rate

3.1.4 Wear test results

Figure 7 shows how the mass wear rate changes with applied stress. It is evident that the wear rate for all applied loads reduces with increasing pressure. Squeeze casting has a substantially lower wear rate than pressure die casting for all applied typical loads. Additionally, the wear rate reduces as the applied pressure at a constant normal load increase. This is because when the applied pressure rises, the material hardens due to decreased shrinkage porosity [21].

Although the friction coefficient decreased, the findings shown in Figure 7 indicate that the addition of nano-Al_2O_3 altered the Al-Si-Cu alloy's wear resistance. Both the high load utilized in the test and microstructural factors may be to blame for the fact that SQ enhanced wear resistance (while increasing hardness and strength) [21]. Higher hardness brought about by Al_2O_3 refinement in microstructural components has been credited with improving the wear resistance of nano-reinforced alloy when compared to non-modified alloy. This behavior is also explained by microstructural impacts in both alloys, where nano additions encourage the production of eutectic Si Al phases while having a more noticeable alteration and refining effect on Al-Si alloys. Tearing and delamination were the primary wear mechanisms seen. Typically, wear testing takes place in a steady-state setting. This is because as sliding time increases, the asperities progressively flatten and expand the true contact area as shown in Figure 8.

3.1.5 Tensile test

The action of the nano alumina in the alloy's eutectic silicon modification makes its analysis difficult. To explain and find the reasons, the high-pressure die casting and squeeze casting simulation results were compared. For easier evaluation and exact interpretation of the alloy structure modification, the AlSiCu with wt% nano alumina alloy samples were produced by squeeze casting. The obtained results revealed that the nano alumina increases the distance between the primary silicon crystals from an average of 3.8 to 4.4 μm and provides several other significant structure modifications, which lead to an increase in the alloy material's mechanical properties. In this investigation, the effect of the nano alumina additive on the properties of the AlSiCu alloy produced by two different high mechanical load-dependent manufacturing technologies – high-pressure die casting and squeeze casting – is made. The mechanical properties, primary and eutectic silicon size, the eutectic silicon volume among the alloy's primary structure, the device-based dependency for the particular construction, and equivalent average values for the Si thickness were compared and evaluated.

Figure 9 displays the Al-Si-Cu's yield strength (YS), ultimate tensile strength (UTS), and strain (El) following the addition of Al_2O_3. The tensile characteristics of Al-Si-Cu in general are greatly influenced by the SDAS structure, which varies with applied pressure. Every sample shown an increase in both final strength and casting (SC and HPDC). Al-Si-Cu alloys can be made stronger by precipitating the Al_2O_3 and Al_2Cu phases. The Al_2Cu phase is aligned with the cube axis <001> of the matrix and has nanoscale dimensions. Numerous studies have examined the impact of crystal and microstructure on solidified deposits [22]. improving mechanical qualities by reducing the size of overlapping fine components (intermetallic or non-metallic inclusions) and encouraging their uniform distribution [23, 24].

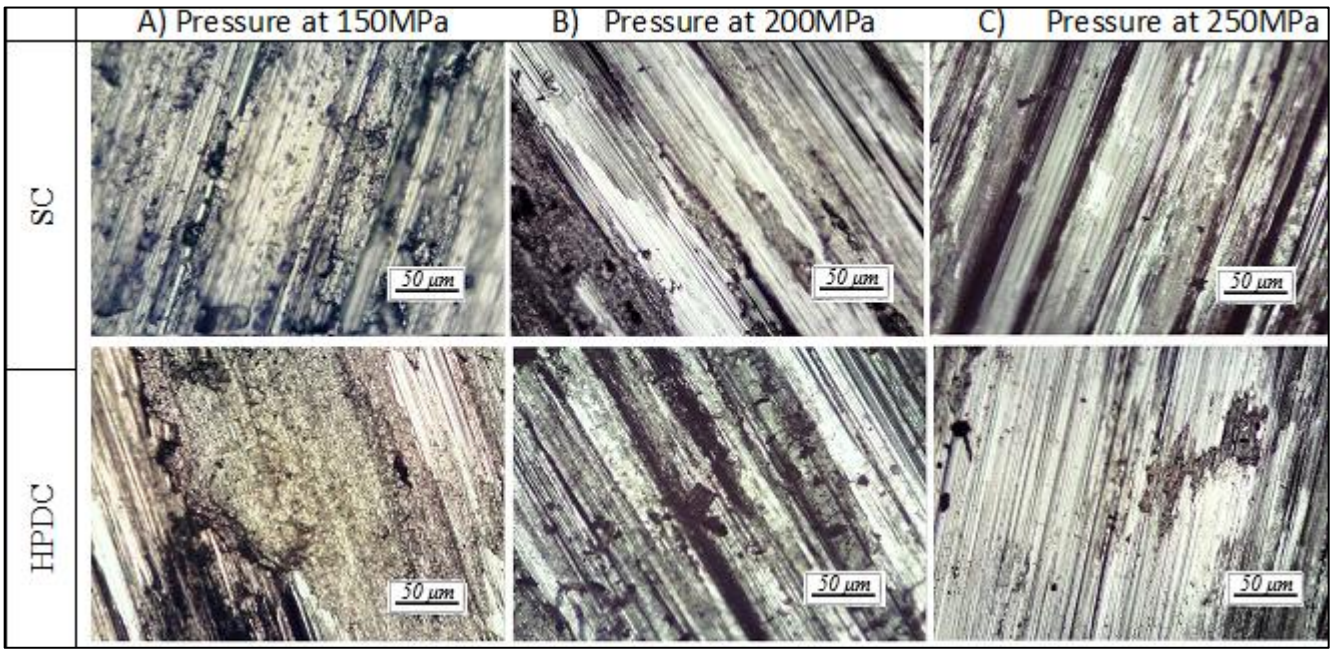

Figure 8. Al-Si-Cu alloys' resistance to wear in relation to applied pressure

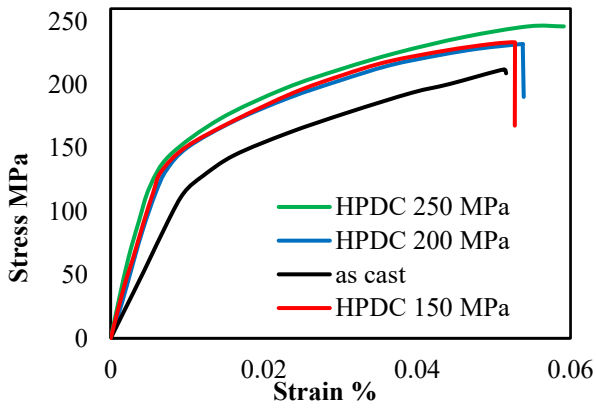

(a) Squeeze casting

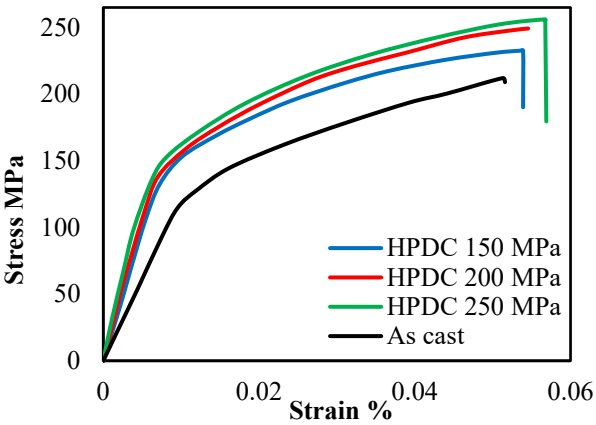

(b) High pressure die casting

Figure 9. After adding Al_2O_3, the Al-Si-Cu's yield strength (YS), ultimate strength (UTS), and strain (El)

3.2 Modeling results

3.2.1 Modeling outcomes

DoE tool examines the observed responses and determines which mathematical models best suit the data. This study employed full factorial design of the experiment that is regarded as the best and most powerful tool in many fields and applications [8-10]. This tool will help to connect the investigated process parameters including nano-percentage additives and the pressure with the main responses including hardness, corrosion, tensile strength, and wear rate of both squeeze casting and HPDC casting. After that, steps have been applied to the techniques to assess the model's adequacy. It also analyzed the impact of process parameters on the selected response to develop the best-fit model. In this part, the relevance between the modeling results will be discussed deeply as follows.

According to the modeling results, it can be seen that both nano-percentage additives and the pressure have a direct impact on the mechanical properties including hardness and tensile strength. Moreover, the nano percentages have the greatest effect than casting pressure as shown in Figures 10(a) and (b). On the other hand, the impact of the nano-additives and casting pressure on the wear and corrosion resistance will be reversed. as it is clear to see in Figures 11(a) and (b) the indirect relationship between them. The previous behavior, which has been shown in Figures 10 and 11 that belonged to the squeeze casting process, completely matches the behavior of the HPDC casting technology regarding the relationship between the invest aged parameters and corresponding responses, see Figures 12 and 13.

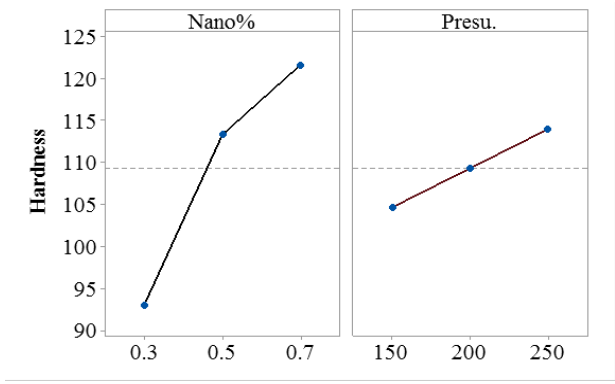

(a) Hardness

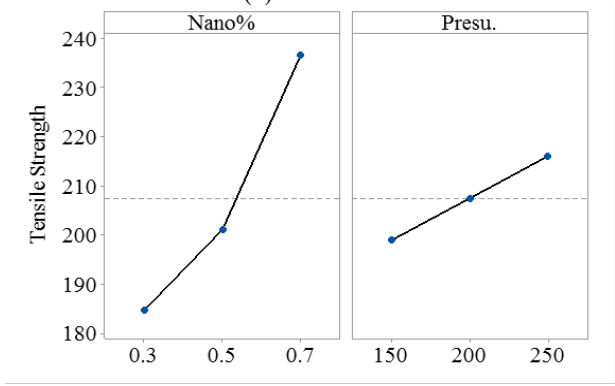

(b) Tensile strength

Figure 10. Main effects of nano addition and casting pressure on squeeze casting

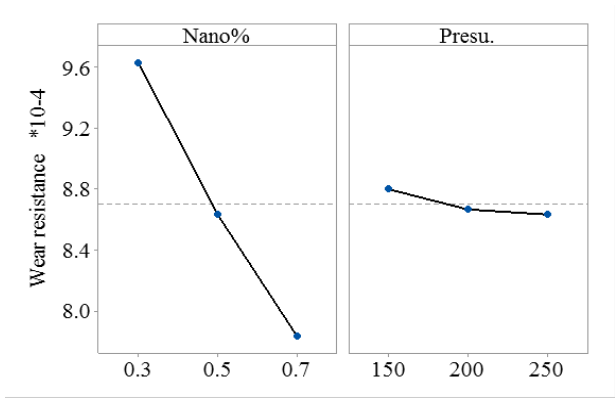

(a) Wear resistance

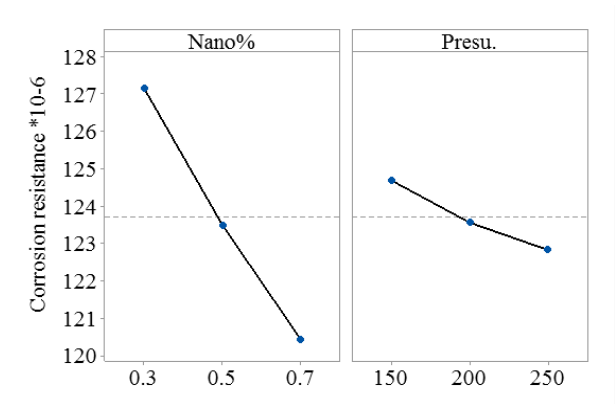

(b) Corrosion resistance

Figure 11. Main effects of nano addition and casting pressure on squeeze casting

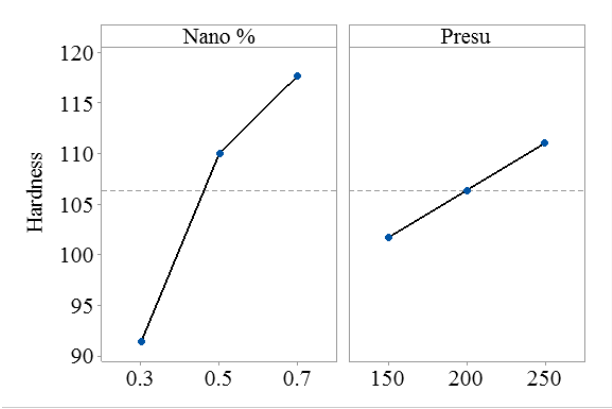

(a) Hardness

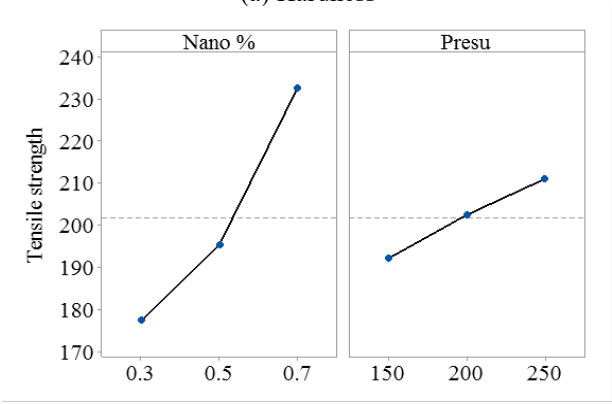

(b) Tensile strength

Figure 12. Main effects of nano addition and casting pressure on HPDC casting

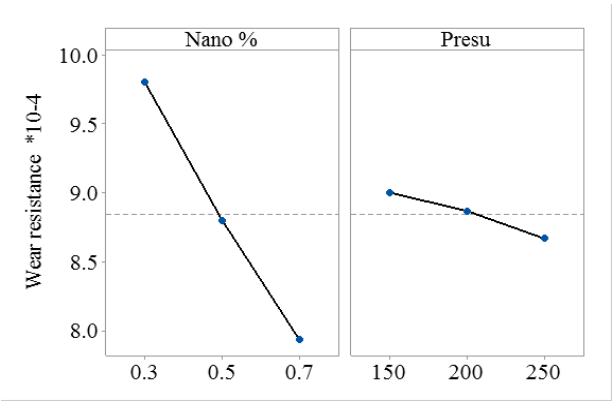

(a) Wear resistance

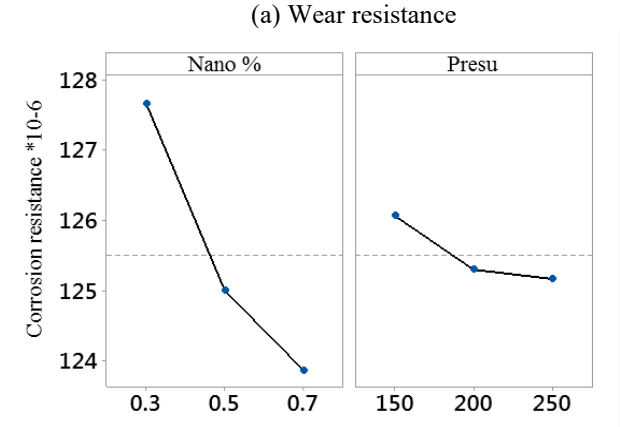

(b) Corrosion resistance

Figure 13. Main effects of nano addition and casting pressure on HPDC casting

One of the most important outcomes of the modeling tools is the final mathematical model that refers to the final equation of the relevance between the process parameters and responses (outputs). The final equations of the responses include hardness, corrosion, tensile strength, and wear rate are shown in the below Eqs. (5)-(8):

$$\text{Hardness} = 54.83 + 71.67\ \text{Nano\%} + 0.0933\ \text{P.} \quad (5)$$

$$\text{Corrosion} *10^{-6} = 135.850 - 16.83\ \text{Nano\%} - 0.01867\ \text{P.} \quad (6)$$

$$\text{Tensile} = 108.2 + 129.8\ \text{Nano\%} + 0.1713\ \text{P.} \quad (7)$$

$$\text{Wear} *10^{-4} = 11.283 - 4.500\ \text{Nano\%} - 0.001667\ \text{P.} \quad (8)$$

It is obvious that the nano-additives have negative effects on wear and corrosion resistance. whereas, it has a positive effect on hardness and strength in inverse to the impact of casting pressure. This corresponded to the previous behaviors that have been seen in Figures 10 to 13.

3.2.2 Model accuracy and validation

Table 3 shows the F and p values results according to the proposed model's ANOVA analysis. The results cover both the DPH and squeeze casting for all the responses involving the hardness, strength, wear, and corrosion resistance. It can be noted that the nano percentage is the first important factor for all the casting types and responses, which matches with the behaviour that has been recorded in Figures 9 to 12 as well as Eqs. (5)-(8). Furthermore, the results regarding the P-value have a maximum value of 0.046, which falls within the acceptable range.

To confirm the model's predictions, the expected outcomes must be contrasted with the testing data in order to take into account any errors that may have been made or the accuracy of the model's predictions. Therefore, as a validation step, the proposed mathematical final models were tested for all run experiments. It has been found that the models of all output responses can predict the responses with an average relative error in the hardness of 1.23. The other errors in other responses were 1.1%, 0.25 and 0.35% for the strength, corrosion, and wear resistance respectively. Figures 14(a)-(d) show the comparison between the experimental runs and the model results. It shows good matching between them for all responses.

Table 3. The results of the proposed model's analysis of Variance (ANOVA), including the F-values and p-values

Parameters		HPDC		Squeeze Casting	
		F-values	p-values	F-values	p-values
Hardness	Model	35.52	0.002	58.19	0.001
	Nano%	63.50	0.001	105.78	0.000
	Pressure	7.54	0.044	10.59	0.025
Tensile Strength	Model	202.31	0.000	78.12	0.000
	Nano%	363.65	0.000	141.50	0.000
	Pressure	40.96	0.002	14.74	0.014
Wear Resistance	Model	304.00	0.000	369.50	0.000
	Nano%	589.00	0.000	732.00	0.000
	Pressure	19.00	0.009	7.00	0.046
Corrosion Resistance	Model	16.19	0.010	61.93	0.001
	Nano%	30.49	0.004	114.92	0.000
	Pressure	1.89	0.026	8.94	0.033

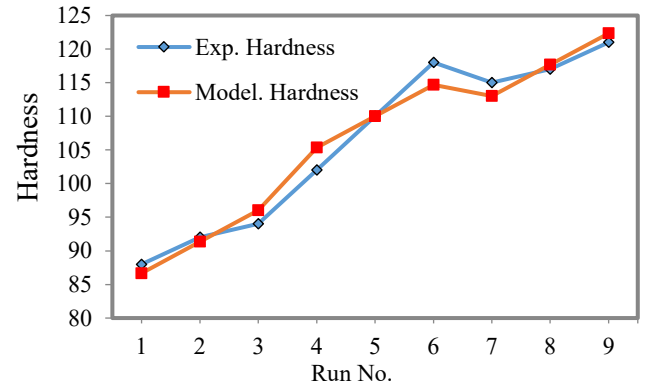

(a) Hardness

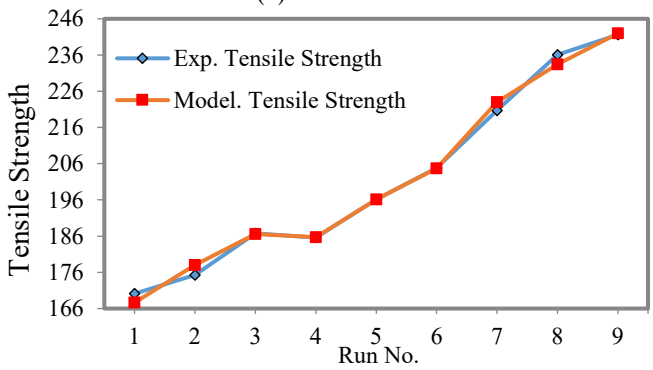

(b) Tensile strength

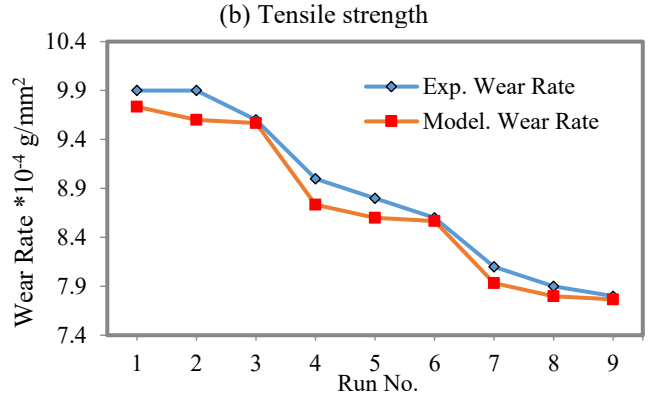

(c) Wear resistance

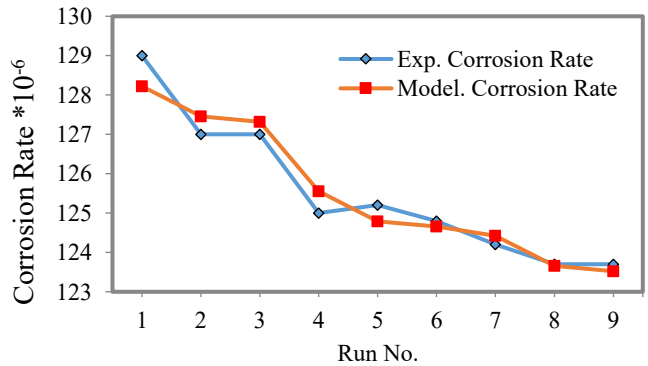

(d) Corrosion resistance

Figure 14. Comparison between experimental and modeling results for HPDC casting for (a) hardness, and (b) tensile (c) wear, and (d) corrosion

The recorded errors by the proposed models of all outputs or responses namely hardness strength, corrosion, and wear resistance are presented in Figures 15 (a) and (b). This Figure 15 demonstrates the individual recorded errors of all responses including hardness, strength, corrosion, and wear resistance for squeeze and pressure casting. Very acceptable recorded errors are presented, making the proposed mathematical model are useful for analysis and optimization.

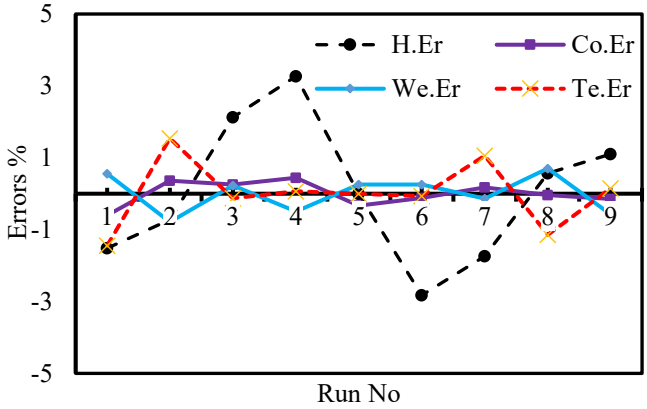

(a) High pressure die casting

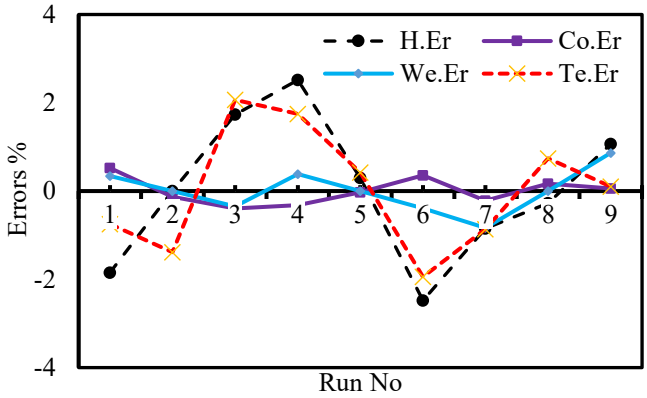

(b) Squeeze casting

Figure 15. Errors levels for (a) HPDC and (b) Squeeze casting

3.2.3 Model analysis

The proposed model could be used to explain and figure out the combined effect of process parameters including Nano-additives, and casting pressure on all responses including hardness, strength, corrosion, and wear resistance for squeeze and pressure casting. First of all, it should be mentioned that the behavior of both the investigated casting processes regarding their relationship with the investigated parameters is the same. For this reason, the analysis will consider only one process namely squeeze casting.

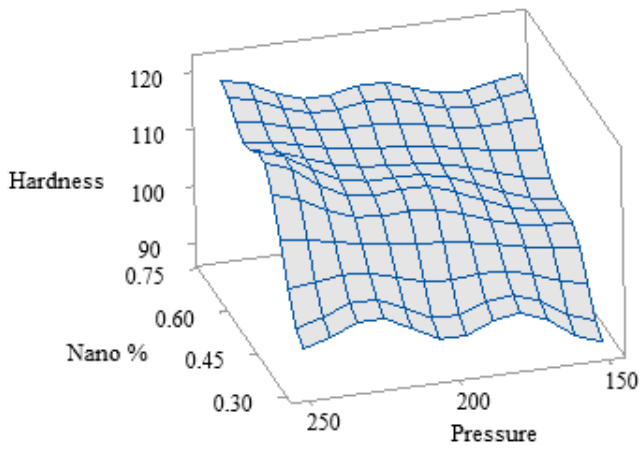

(a) Hardness

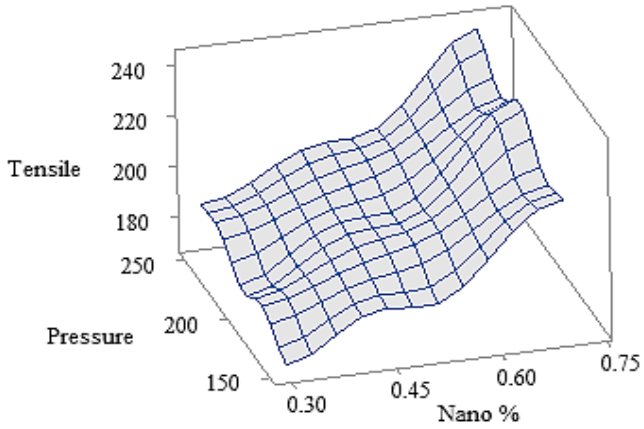

(b) Strength

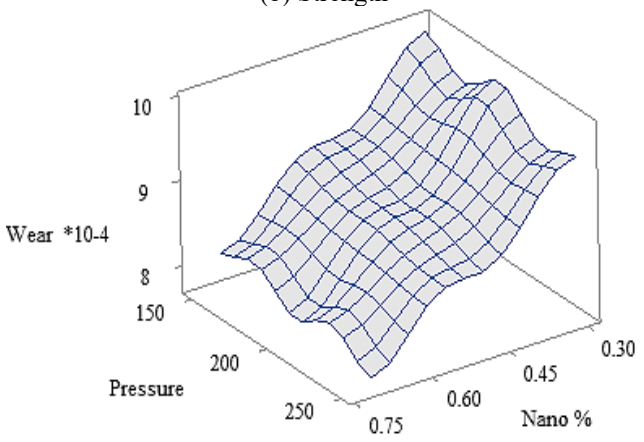

(c) Wear resistance

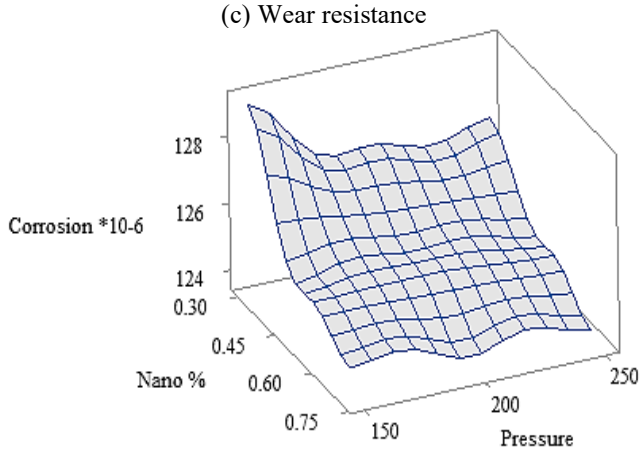

(d) Corrosion resistance

Figure 16. The combined effect of nano additives and casting pressure

Figures 16 (a)-(d) demonstrate the combined impact of process parameters on the responses. Where Figure 16 (a) shows the effect of both nano additives and casting pressure on the hardness. According to this Figure, maximum product hardness could be achieved by setting the nano additives and casting pressure at maximum values. The same requirements are required to increase the strength, as it can be noted in Figure 16 (b). On the other hand, the setup of nano additives and casting pressure at minimum values reduces the corrosion and wear resistance to minimum, see Figures 16 (c) and (d).

4. CONCLUSIONS

The present research investigates the possibility of a modification of a real nominal Al-Si-Cu alloys using nano-scale Al_2O_3 particles. The role of nanosized oxide particles during solidification and their effect on the melt structure condition were studied.

1- A melt comprising Al_2O_3 nano powder at 780°C and its interaction. An "in situ" metal volume is uniformly dispersed with aluminum oxide nanoparticles that are completely wetted by aluminum. The mass fraction of eutectic aluminum increases up to 26 weight percent as a result of the concentration, which is dependent on the pressure holding time in the melt.

2- In uniaxial tension, it was found that squeeze casting greatly increased the tensile strength, yield strength, hardness, and ductility of cast Al-αnano-Al_2O_3 composites (1.2-1.6 times), while HPDC increased them (1.2-1.8 times) with increasing pressure. The composites with 0.7 weight percent have the highest tensile strength. Alongside this notable rise in tensile strength, the nanocomposite's elongation also significantly increases. The development of a very tiny, uniformly distributed, and thoroughly wetted aluminum nano oxide within an aluminum matrix is what causes this combination of mechanical qualities.

3- Because of its nano-AlO_3, this system is a very appealing structural material that is elastic, hard, strong, and light.

4- mechanism via which the addition of genuine aluminum oxide nanoparticles to the Al-AlO_3 composite results in a simultaneous improvement in mechanical characteristics and corrosion resistance.

5- Adding Al_2O_3 nanoparticles improved the wear resistance of composite components. The delamination and shallow plowing grooves demonstrate that the predominant wear process was a mix of adhesion and delamination.

REFERENCES

[1] Zhang, Y.B., Wang, W., Liu, J.J., Wang, T.M., Li, T.J. (2023). Fabrication of carbon fiber reinforced aluminum matrix composites by inorganic binders. Journal of Alloys and Compounds, 968(15): 172213. https://doi.org/10.1016/j.jallcom.2023.172213

[2] Berlanga-Labari, C., Biezma-Moraleda, M.V., Rivero, P.J. (2020). Corrosion of cast aluminum alloys: A review. Metals, 10(10): 1384. https://doi.org/10.3390/met10101384

[3] Zhang, J., Hu, J., Lu, Y.L., Gu, J.Y., Yang, X.H., Zhao, Y.C., Qi, L., Wei, W. (2025). The enhancement of corrosion resistance for Al-Cu alloy reinforced by ZrB2 particles with different scales. Journal of Alloys and Compounds, 1026(5): 180357. https://doi.org/10.1016/j.jallcom.2025.180357

[4] Manani, S., Patodi, A., Verma, M.N. Pradhan, A.K. (2022). Comparative study of microstructure and properties of hypoeutectic Al-Si alloys being cast with and without melt thermal treatment. Metallography, Microstructure, and Analysis, 11: 415-424. https://doi.org/10.1007/s13632-022-00855-w

[5] Singh, L., Sehgal, S., Saxena, K.K. (2021). Behaviour of Al_2O_3 in aluminium matrix composites: An overview. E3S Web of Conferences, 309: 01028. https://doi.org/10.1051/e3sconf/202130901028

[6] Yildirim, M., Özyürek, D., Tunçay, T. (2017). The Effects of molding materials on microstructure and wear behavior of A356 alloy. High Temperature Materials and Processes, 36(5): 515-521. https://doi.org/10.1515/htmp-

2015-0240
[7] Bogdanoff, T., Dahlström, J. (2009). The influence of copper on an Al-Si-Mg alloy (A356) - Microstructure and mechanical properties. Digitala Vetenskapliga Arkivet.
[8] Guo, M.H., Sun, M., Huang, J.H., Pang, S. (2022). A comparative study on the microstructures and mechanical properties of Al-10Si-0.5Mg alloys prepared under different conditions. Metals, 12(1): 142. https://doi.org/10.3390/met12010142
[9] Jamwal, A., Vates, U.K., Gupta, P., Aggarwal, A., Sharma, B.P. (2019). Fabrication and characterization of Al_2O_3–TiC-Reinforced aluminum matrix composites. Advances in Industrial and Production Engineering, 349-356. https://doi.org/10.1007/978-981-13-6412-9_33
[10] Bachy, B. (2023). Laser micro-drilling process: Experimental investigation, modeling based on RSM-BBD tool and multi-criteria optimization. Journal of the Brazilian Society of Mechanical Sciences and Engineering, 45(3): 180. https://doi.org/10.1007/s40430-023-04112-1
[11] Hussein, S.A., Bachy, B.S. (2024). Evaluation of joint strength in laser transmission welding of PMMA polymer. Association of Arab Universities Journal of Engineering Sciences, 31(4). https://doi.org/10.33261/jaaru.2024.31.4.002
[12] Xing, Y.T., Zhang, X.X., Ma, Y.W., Tian, Z.R., Li, X., Yu, J.B., Xuan, W.D., Ren, Z.M. (2025). Optimization of die casting process and microstructure-mechanical properties of Al-Sc alloys. International Journal of Material Forming, 18: 26. https://doi.org/10.1007/s12289-025-01885-9
[13] Othman, K., Ghani, J.A., Juri, A., Mohd, S., Kasim, M.S., Haron, C.H.C. (2020). Optimization of tool life and surface roughness for hypereutectic Al-Si alloys in face milling. Journal of Mechanical Engineering, 17(2): 27-44. https://doi.org/10.24191/jmeche.v17i2.15299
[14] Hussein H.A., Khanjar R.H., Hussein, S.G. (2023). Evaluation of physical characterizations of an Al-matrix composite material enhanced with TiO_2 particles manufactured by powder technique. In 8th Engineering and 2nd International Conference for College of Engineering – University of Baghdad: Coec8-2021 Proceedings, Baghdad, Iraq. https://doi.org/10.1063/5.0105419
[15] Hussein, H.A., Kahdim, M.J., Atiyah, A.A. (2020). Microstructural modifications produced by nano-metal-phosphate additions to aluminum-silicon alloy by new system projects. Journal of Physics: Conference Series, 1773(1): 012024. https://doi.org/10.1088/1742-6596/1773/1/012024
[16] Taufikurrahman, Y Nukman, Yanis, M. (2013). Effect of the pressure of the squeeze process on the hardness and micro structure of recycled aluminum materials. Journal of Mechanical Science and Engineering, 1(1). https://jmse.ejournal.unsri.ac.id/index.php/jmse/article/view/2.
[17] Yolshina, L., Kvashnichev, A., Vichuzhanin, D., Smirnova, E. (2022). Mechanical properties of aluminum matrix composites reinforced by in situ Al2O3 nanoparticles fabricated via direct chemical reaction under salt flux. Social Science Research Network. https://papers.ssrn.com/sol3/papers.cfm?abstract_id=4017473.
[18] Boschetto, A., Costanza, G., Quadrini, F., Tata, M.E. (2007). Cooling rate inference in aluminum alloy squeeze casting. Materials Letters, 61(14-15): 2969-2972. https://doi.org/10.1016/j.matlet.2006.10.048
[19] Obiekea K., Aku S.Y., Yawas D.S. (2012). Influence of pressure on the mechanical properties and grain refinement of die cast aluminum A1350 alloy. Advances in Applied Science Research, 3(6): 3663-3673.
[20] Rosliza, R. (2012). Improvement of corrosion resistance of aluminium alloy by natural products. In Corrosion Resistance. https://doi.org/10.5772/32952
[21] Hussein, H.A., Kahdim, M.j., Atiyah, A.A. (2020). Effects of new modification and refinement techniques of mechanical properties and corrosion behaviours of al-si alloys. IOP Conference Series: Materials Science and Engineering, 987(1): 012014. https://doi.org/10.1088/1757-899X/987/1/012014
[22] Wan Nik, W.B., Sulaiman, O., Fadhli, A., Rosliza, R. (2010). Corrosion Behavior of aluminum alloy in seawater. In the International Conference on Marine Technology, Dhaka, Bangladesh, pp. 175-180.
[23] Gürbüz, M., Şenel, M.C. (2019). Fabrication and mechanical behavior of aluminum matrix composites reinforced with nano alumina particles. Duzce University Journal of Science and Technology, 7(3): 1341-1350. https://doi.org/10.29130/dubited.518527
[24] Rathod, L., Purohit, G.K. (2013). A study of microstructure and mechanical property of aluminum-alumina metal matrix. International Journal of Engineering Research & Technology (IJERT), 2(9).